The Hydrodynamic Deviation of Earth's Collisionless Bow Shock

Becca Lindenbaum[a], Colby Haggerty[b]

[a]*Haverford College, 370 Lancaster Ave., Haverford, PA 19041, USA*

[b]*Institute for Astronomy, University of Hawai'i, 2680 Woodlawn Drive, Honolulu, HI 96822, USA*

Abstract

Earth's bow shock is a standing shock wave where the Earth's magnetosphere meets the solar wind, a collisionless, super-sonic plasma coming from the sun. At the bow shock, solar wind plasma is heated, compressed and energized before it interacts with the magnetosphere. The physics and predictions for the bow shock have been primarily considered using a fluid, magneto-hydrodynamic (or MHD) description, despite the fact that the conditions of the bow shock violate the basic assumptions of MHD. Motivated by recent advances in kinetic plasma theory, we use high cadence, multi-point measurements of the magnetic fields and plasma quantities made by NASA's Magnetospheric Multiscale (MMS) satellites at Earth's bow shock to test if the predictions of MHD are applicable for this system. We find that the compression ratio measured by MMS has little to no correlation with the MHD predictions and we investigate different possible explanations for this deviation. These findings have important implications for the interaction of solar wind and the magnetosphere, as well as for space weather modeling more generally.

Keywords: bow shock, upstream, downstream, sonic mach number, alfvén speed

1. Introduction

Shocks are disturbances that move faster than the local speed of sound in the medium, and cause a change in density. When shocks are collisionless, the mean free path of a particle is much larger than the transition from pre-shock to post-shock. Bow shock is a collisionless shock that occurs when the magnetosphere of an object interacts with flowing plasma.

Shock waves, as shown in Figure 1 have upstream and downstream components. Incoming particles are the 'upstream' of the shock, before interacting with it, and typically have faster speeds and lower spatial density. The outgoing particles are the 'downstream' of the shock, and typically have slower velocity and higher spatial density.

Email address: blindenbau@haverford.edu (Becca Lindenbaum)

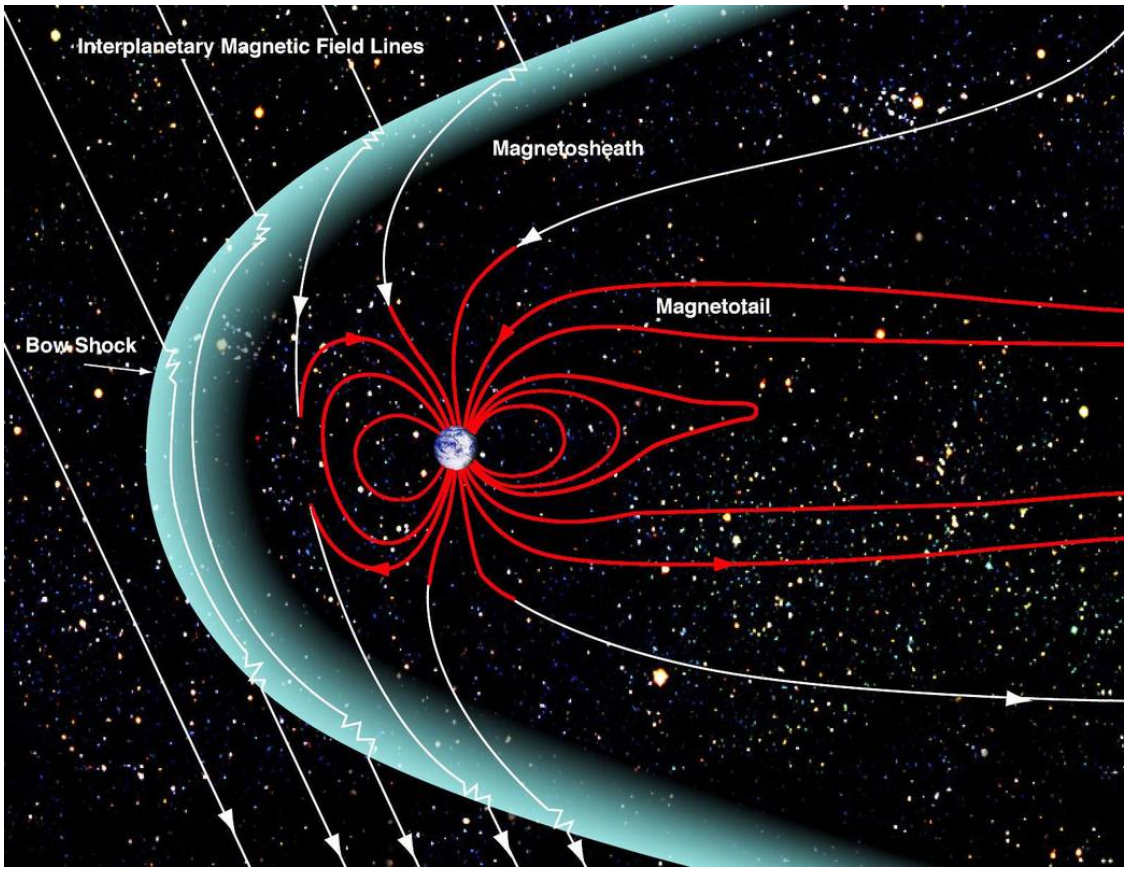

Figure 1: NASA depiction of Earth's magnetosphere and bow shock

There are two main types of shocks, quasi-perpendicular and quasi-parallel. Quasi-perpendicular shocks occur when the flow and magnetic field are perpendicular to each other, and quasi-parallel shocks occur when the flow and magnetic field are parallel (or anti-parallel) to each other. Quasi-parallel shocks can be reflected back upstream, and can cause instabilities.

Collisionless shocks are plentiful in astrophysical plasmas, and Earth's bow shock is an example of this. Solar wind, a stream of charged particles from the sun's corona, interacts with Earth's magnetosphere to cause this shock. Most of the understanding of how these plasma shocks work is from fluid Rankine–Hugoniot jump conditions, which are collisional.

Nonrelativistic shocks can transfer up to 20% of their ram energy into non-thermal particles (Krymskii, 1977), which can cause plasma instabilities in the upstream of the shock (Bell, 2004).

Non-thermal particles can take energy away from the shock at an enhanced rate. Haggerty and Caprioli (2020) suggest that non-thermal particles remove energy from the shock at an enhanced rate which should change the shock's hydrodynamics. While this has been found in kinetic simulations, and agrees with astrophysical observations of hadronic emission, it has not been verified by observations. This work aims to address this from direct observations

of Earth's bow shock with MMS.

We calculate the shock's compression ratio as the ratio of the upstream and downstream electron number densities. Traditionally, the compression ratio is thought of to be

$$r = \frac{(\Gamma + 1)M_1^2}{2 + (\Gamma - 1))M_1^2} \quad (1)$$

where the data approaches 4, but does not go over it, and is dependent on the magnetosonic Mach number, the speed at which the particles in the plasma are traveling relative to the speed of sound in the medium. However, the traditional model is based on MHD which assumes that collisions are frequent, while Earth's bow shock is collisionless.

In this paper, we test the findings of the simulations done by Haggerty and Caprioli, 2020, using data from the four Magnetospheric Multiscale (MMS) spacecraft, (Pollock et al., 2016), only using measurements that occur close to the bow shock.

The layout of this paper is as follows: in Section 2, we detail the MMS instruments and observations. In Section 3, we present the results, and finally, in Section 4, we discuss the implications of our research and discoveries to the dynamics and our current understanding of collisionless plasma shocks.

2. MMS Observations

2.1. Data

We use data from the Magnetospheric Multiscale (MMS) spacecrafts, primarily from MMS1. The MMS Mission is a NASA robotic space mission used to study Earth's magnetosphere, using four identical spacecraft flying in a tetrahedral formation. It was launched in March 2015 and measures magnetic field lines and charged particles in the magnetosphere.

Ion moments and distribution functions are from the Fast Plasma Investigation Dual Ion Spectrometer (FPI-DIS), and electron moments and distribution functions are from the Fast Plasma Investigation Dual Electron Spectrometer (FPI-DES). The energy range of the ion measurements used here are from 2–18 keV, and 28 keV during different times. FPI observes fast-moving plasma. Incoming particles pass through a filter which takes certain particle speeds and directions and passes them through to a sensor plate. When a particle hits the sensor plate, millions of electrons come out the other side, so the instrument can detect the event, which takes several nanoseconds. FPI separately measures electrons and ions, and can count the number of particles of each kind entering the instrument. Four sensors are used to detect the electrons and another four for the ions. Each sensor is made of two spectrometers whose field of view is separated by 45 degrees, each of which can scan through a 45-degree arc for a larger panorama, so together the sensors can observe the entire sky.

Magnetic field data are from the FluxGate Magnetometer (FGM) instrument, which provides magnetic field vector measurements at a resolution of 128 Hz (Russell et al., 2016). The FGM

instrument has three data acquisition rates, slow survey, fast survey and burst. Burst rates only save the most scientifically interesting time segments. Fast survey data are collected simultaneously with burst data, and are used to refine the selection of burst data segments, while slow survey data has minimized sampling rates to reserve data storage but cover longer periods of time (Baker et al., 2016). We use survey data, as the data collected from burst mode are just the bow shock, but not the data from before and after the shock occurs.

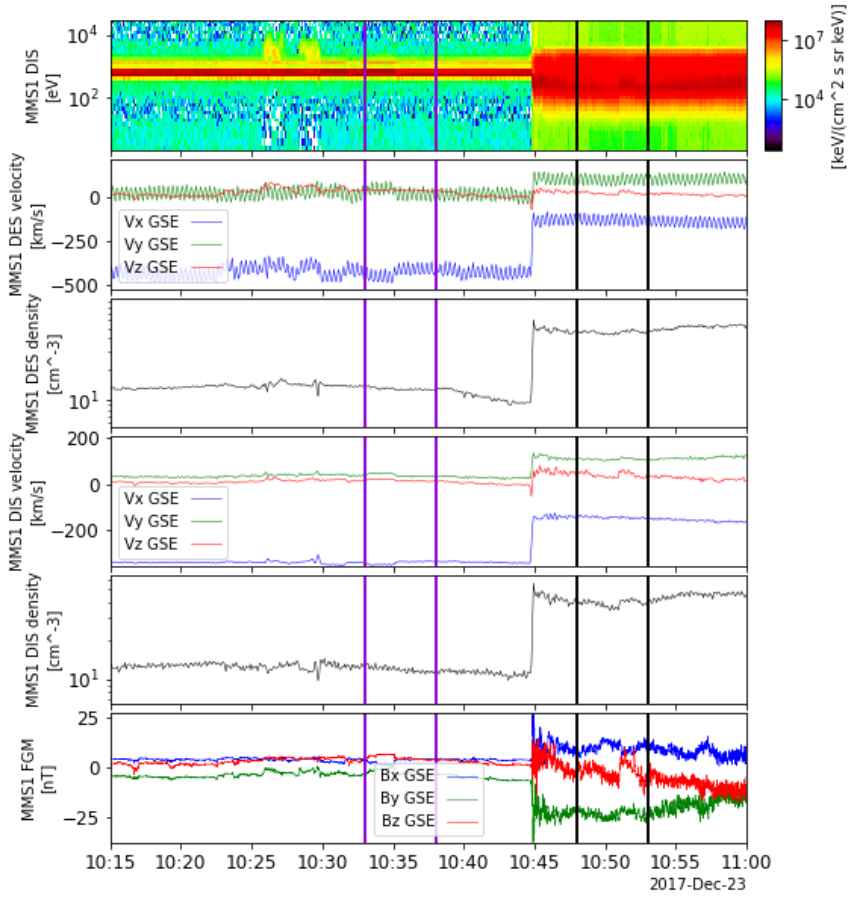

Figure 2: December 23, 2017, from 10:00 to 11:00, the five minute window for the upstream is indicated with the black lines and the five minute window for the downstream is indicated with the purple lines. (from bottom to top) ion energy spectra, electron bulk velocity, electron number density, ion bulk velocity, ion number density, and the magnetic field in the given times. The different colors for bulk velocity and magnetic field are for the x, y, and z directions, where x is blue, y is green, and z is red. The color variation in the energy spectra graph depicts the irradiance.

All upstream solar-wind parameters are from OMNI, a set of spacecraft positioned upstream of MMS at the first Lagrange point. The solar-wind data are time shifted to the bow shock and provided by the OMNI database with a time resolution of one minute (King and Papitashvili, 2005).

We perform a statistical study using encounters with the bow shock by the MMS spacecraft.

The encounters occurred between October 2017 and April 2018 during a period when MMS crossed the bow shock every orbit. This time interval is close in time to solar minimum, which reduces the risk of energetic ions from the Sun or geomagnetic storms.

We wanted to look at times close to the bow shock, but wanted the data to be fairly constant. The graph shown in Figure 2 show an example of the data surrounding the bow shock.

The equation for the magneto-sonic Mach number is

$$M_s = \frac{v_{up}}{v_{sound}} = \frac{v_{up}}{\sqrt{\Gamma T/m_i}} \tag{2}$$

where M_s is the sonic mach number, v_{up} is the upstream velocity, v_{sound} is the speed of sound, and v_A is the upstream alfvén velocity. Γ is 5/3, the constant for a monoatomic ideal gas, T is the temperature, and m_i is the mass of an ion.

Our temperature and density data was cross-referenced with OMNI data, as MMS does not have accurate temperature data.

We took nine quasi-parallel shock crossings and calculated the compression ratio using electron number density from the upstream and downstream, and the magnetosonic mach number from the research of Johlander et al. (2021). 3 demonstrates this relationship.

3. Results and Discussion

As shown in 3, the relationship between the compression ratio and the supersonic Mach number does not match traditional MHD predictions.

4. Conclusions

In this work, we studied a collection of shock crossings by the MMS spacecraft.

It is unclear if MHD is a good depiction for the bow shock.

It is important to note that there are limitations to what can be done with MMS for studying the bow shock.

Acknowledgements

We would like to thank A. Johlander for his list of shock crossings.

We are thankful for the dedicated efforts of the entire MMS mission team, including development, science operations, and the Science Data Center at the Univ. of Colorado for access and support. The data presented in this paper are the L2 data of MMS and can be accessed from MMS Science Data Center (`https://lasp.colorado.edu/mms/sdc/public/`).

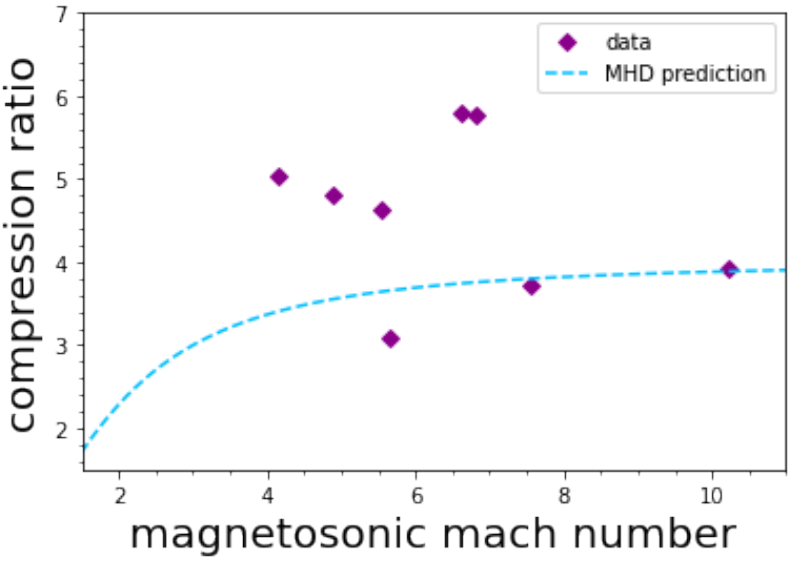

Figure 3: the compression ratio vs supersonic mach number for eight quasi-perpendicular shock crossings, measured with MMS and OMNI data. The calculated values are larger than traditional MHD predictions.

The OMNI data were obtained from the GSFC/SPDF OMNIWeb interface at `https://omniweb.gsfc.nasa.gov`.

Becca Lindenbaum acknowledges support from Research Experience for Undergraduate program at the Institute for Astronomy, University of Hawaii-Manoa funded through NSF grant #2050710.

Becca Lindenbaum would like to thank the Institute for Astronomy for their hospitality during the course of this project.

Dr. Haggerty acknowledges the support of NSF FDSS grant AGS-1936393

References

D. N. Baker, L. Riesberg, C. K. Pankratz, R. S. Panneton, B. L. Giles, F. D. Wilder, and R. E. Ergun. Magnetospheric Multiscale Instrument Suite Operations and Data System. Space Sci. Rev., 199(1-4): 545–575, Mar. 2016. doi: 10.1007/s11214-014-0128-5.

A. R. Bell. Turbulent amplification of magnetic field and diffusive shock acceleration of cosmic rays. *Monthly Notices of the Royal Astronomical Society*, 353(2):550–558, 09 2004. ISSN 0035-8711. doi: 10.1111/j.1365-2966.2004.08097.x. URL `https://doi.org/10.1111/j.1365-2966.2004.08097.x`.

C. C. Haggerty and D. Caprioli. Kinetic simulations of cosmic-ray-modified shocks. i. hydrodynamics. *The Astrophysical Journal*, 905(1):1, dec 2020. doi: 10.3847/1538-4357/abbe06. URL `https://doi.org/10.3847/1538-4357/abbe06`.

A. Johlander, M. Battarbee, A. Vaivads, L. Turc, Y. Pfau-Kempf, U. Ganse, M. Grandin, M. Dubart, Y. V. Khotyaintsev, D. Caprioli, C. Haggerty, S. J. Schwartz, B. L. Giles, and M. Palmroth. Ion acceleration efficiency at the earth's bow shock: Observations and simulation results. *The Astrophysical Journal*, 914 (2):82, jun 2021. doi: 10.3847/1538-4357/abfafc. URL `https://doi.org/10.3847/1538-4357/abfafc`.

J. H. King and N. E. Papitashvili. Solar wind spatial scales in and comparisons of hourly Wind and ACE plasma and magnetic field data. *Journal of Geophysical Research (Space Physics)*, 110(A2):A02104, Feb. 2005. doi: 10.1029/2004JA010649.

G. F. Krymskii. A regular mechanism for the acceleration of charged particles on the front of a shock wave. *Akademiia Nauk SSSR Doklady*, 234:1306–1308, June 1977.

C. Pollock, T. Moore, A. Jacques, J. Burch, U. Gliese, Y. Saito, T. Omoto, L. Avanov, A. Barrie, V. Coffey, J. Dorelli, D. Gershman, B. Giles, T. Rosnack, C. Salo, S. Yokota, M. Adrian, C. Aoustin, C. Auletti, S. Aung, V. Bigio, N. Cao, M. Chandler, D. Chornay, K. Christian, G. Clark, G. Collinson, T. Corris, A. De Los Santos, R. Devlin, T. Diaz, T. Dickerson, C. Dickson, A. Diekmann, F. Diggs, C. Duncan, A. Figueroa-Vinas, C. Firman, M. Freeman, N. Galassi, K. Garcia, G. Goodhart, D. Guererro, J. Hageman, J. Hanley, E. Hemminger, M. Holland, M. Hutchins, T. James, W. Jones, S. Kreisler, J. Kujawski, V. Lavu, J. Lobell, E. LeCompte, A. Lukemire, E. MacDonald, A. Mariano, T. Mukai, K. Narayanan, Q. Nguyan, M. Onizuka, W. Paterson, S. Persyn, B. Piepgrass, F. Cheney, A. Rager, T. Raghuram, A. Ramil, L. Reichenthal, H. Rodriguez, J. Rouzaud, A. Rucker, Y. Saito, M. Samara, J. A. Sauvaud, D. Schuster, M. Shappirio, K. Shelton, D. Sher, D. Smith, K. Smith, S. Smith, D. Steinfeld, R. Szymkiewicz, K. Tanimoto, J. Taylor, C. Tucker, K. Tull, A. Uhl, J. Vloet, P. Walpole, S. Weidner, D. White, G. Winkert, P. S. Yeh, and M. Zeuch. Fast Plasma Investigation for Magnetospheric Multiscale. Space Sci. Rev., 199(1-4):331–406, Mar. 2016. doi: 10.1007/s11214-016-0245-4.

C. T. Russell, B. J. Anderson, W. Baumjohann, K. R. Bromund, D. Dearborn, D. Fischer, G. Le, H. K. Leinweber, D. Leneman, W. Magnes, J. D. Means, M. B. Moldwin, R. Nakamura, D. Pierce, F. Plaschke, K. M. Rowe, J. A. Slavin, R. J. Strangeway, R. Torbert, C. Hagen, I. Jernej, A. Valavanoglou, and I. Richter. The Magnetospheric Multiscale Magnetometers. Space Sci. Rev., 199(1-4):189–256, Mar. 2016. doi: 10.1007/s11214-014-0057-3.